# Apparatus for Studying Human Perception of Luminaire Luminance Uniformity

Benjamin Feagin Jr.
Lia Irvin
Eduardo Rodriguez-Feo Bermudez
Michael Royer

Pacific Northwest National Laboratory
620 SW 5th Avenue, Suite 810
Portland, OR 97204
benjamin.feagin@pnnl.gov

**This is an archival copy of an article published in *Proceedings of the 2020 Illuminating Engineering Society Annual Conference*. Please cite as:**

Benjamin Feagin Jr., Lia Irvin, Eduardo Rodriguez-Feo Bermudez, Michael Royer, "Apparatus for Studying Human Perception of Luminaire Luminance Uniformity," *Proceedings of the 2020 Illuminating Engineering Society Annual Conference*

# Apparatus for Studying Human Perception of Luminaire Luminance Uniformity

Benjamin Feagin Jr.*[1], Lia Irvin[1], Eduardo Rodriguez-Feo Bermudez[1], Michael Royer[1]

[1]Pacific Northwest National Laboratory

*benjamin.feagin@pnnl.gov (ORCID: 0000-0001-5484-344X)

**ABSTRACT**

The Luminaire Luminance Uniformity Apparatus was designed to facilitate human factors investigations of perceived luminance uniformity of luminaire apertures, with the goal of developing luminance uniformity metrics tailored to this application. This article documents the design and key features of the apparatus, which consists of three main parts, the Unit Under Test Bisection, Measurement Device Bisection, and a Unified Control Module. The Unit Under Test Bisection hosts mock luminaire configurations as stimuli for human psychophysical experiments or luminance measurement. The Measurement Device Bisection hosts rotating and linear stages to accurately position devices for a variety of luminance measurement methods. The Unified Control Module provides all power and data requirements of the two bisections from a central location. This new apparatus will enable new research on perceived luminance uniformity through automated user-control of the distance between an LED array and optical material, manual selection of optical materials, and an automated system that rapidly obtains precise luminance measurements with multiple devices and methods.

## 1) INTRODUCTION

Technological advances in LEDs and optical materials have created new opportunities to optimize luminaires for efficacy, cost, and user acceptance of visual appearance. For some luminaires, user acceptance depends on the perceived uniformity of the luminance pattern produced by the optical materials at the luminaire aperture. While the IES provides guidance on illuminance uniformity and luminance ratios for establishing contrast (DiLaura, et al., 2011), there are no standardized methods for measuring detailed luminance patterns of an area nor metrics for assessing luminance uniformity that are based on human perception.

Some work has examined the perception of luminance patterns (Zhang & Ngai, 1993; Tang, 1996; Wang & Davis, 1996; Davis & Spring, 2007; Moreno, 2010; Ashdown, 2013), including at least one study on the uniformity of simulated patterns (Yao, et al., 2017). This body of work suggests that basic measures, such as maximum to minimum (max:min) luminance ratios, do not reflect how the human visual system processes luminance patterns. New measures of luminance uniformity are needed to properly assess the uniformity of an area.

Both to develop and make use of new measures of luminance uniformity, procedures for accurately measuring detailed luminance patterns of an area are needed. Luminance uniformity measurement methods from the flat-panel display industry are observed to be a common reference point, for which Downen (2006) provided a state-of-the-art review of existing

measurement methods from the Video Electronic Standards Association (VESA), the International Organization for Standardization (ISO), Swedish Confederation of Professional Employees (TCO), and the Standard Panels Working Group (SPWG) (VESA, 2001; ISO, 2001; TSO, 2005; SPWG, 2005). One commonality of the reviewed methods was a limited quantity of measurement targets at specified positions, with each measurement obtained from a perpendicular point (an infinity perspective). These measurements were then quantified in the form of maximum-to-minimum (max:min) ratio. While newer versions of these documents are available, the emphasis on this methodology has not changed. Standards from the television broadcast industry reflect these same methods (EBU, 2008).

For nearly-Lambertian surface visual displays where luminance of the surface is isotropic, measured from an infinity perspective, the procedures are acceptable. When applied to luminaire apertures that are less Lambertian than visual displays, however, the procedures can introduce additional uncertainty, as represented in Yu and Chung (2011, p. 409): "*The results … show that the more the source is unlike a Lambertian source …, the greater the effect of the measurement method on the measurement results*." There are characteristics of luminance distribution that vary when observing the luminaire aperture from a point, such as the point of view of a human eye, where the direction of view is non-orthogonal to many points on the plane of the aperture.

Resolving this issue of perspective for luminance meter measurement within the flat-panel display industry, ISO (2001) had procedures for obtaining measurements by rotating about a "design-eye point," which has continued to develop over time (ISO, 2008). SID (2012) also provides an option of obtaining luminance meter measurements by rotating about a point instead of an infinity perspective, when an observer might view the display up close. EBU (2008) is also being revised to accommodate new high-dynamic-range (HDR) methods of measuring luminance, which will also accommodate a single observation point. While HDR may be a successful technology in the future, the many sources of error have not been well quantified and controlled (Inanici, 2006; Safranek & Davis, 2020), placing additional emphasis on developing methods utilizing spectroradiometers or luminance meters.

The use of a limited number of measurement points and an assumed infinity perspective are hypothesized to be insufficient for characterizing the perceived uniformity of luminaire apertures, because observers in buildings are not at an infinite distance from non-Lambertian surface luminaires. The Luminaire Luminance Uniformity Apparatus (LLUA) was developed in response to the challenges of assessing luminaire luminance uniformity within the architectural lighting industry, including the need to develop both uniformity metric(s) and luminance uniformity measurement techniques. The LLUA was also designed to facilitate human psychophysical experiments on perceived luminaire aperture luminance uniformity for mock luminaire configurations, collecting corresponding luminance measurements from a variety of measurement devices. The details of how collected data from this apparatus translates to luminance uniformity metrics is detailed in a separate technical paper (Irvin, et al., 2020). This paper focuses solely on the design and development of the apparatus.

## 2) THE LUMINAIRE LUMINANCE UNIFORMITY APPARATUS (LLUA)

The LLUA enables investigation of perceived luminaire luminance uniformity with a physical apparatus (*e.g.*, real optical materials and luminance distributions), as opposed to simulation on a computer display. The LLUA was designed and constructed to vary parameters that have been identified as potential contributors to perceived luminaire luminance uniformity:

- On-center distance between individual LED mounting locations (*i.e.*, pitch)
- LED source mounting arrangement (*e.g.*, rectilinear array)
- Luminance of the LED source(s)
- Distance between the LED source(s) and a remote optical material (*e.g.*, diffuser or lens)
- Remote optical material properties (*e.g.*, bi-directional transmission distribution)
- Distance between the optical material and the observer or measurement device
- Measurement device or observer

The apparatus is comprised of three major subassemblies and some ancillary adjoining components (Figure 1):

- Unified Control Module (UCM)
- Unit Under Test Bisection (UUTB)
- Measurement Device Bisection (MDB)


*Figure 1. Luminaire Luminance Uniformity Apparatus (LLUA) subassembly identification.*

The frame and panels of the UUTB and MDB are constructed of 80/20® Inc. components, with 0.04m (1.50") square ultra-light aluminum extrusions. The frame was designed to minimize deflection and vibration during motorized movement of cantilevered components. The frame

and panels of the UCM are also constructed of 80/20® Inc. components, but with 1" square aluminum extrusions.

The UCM contains all the power supplies and control electronics for the apparatus (see Section 2.1). The UUTB functions as a customizable 0.61m × 0.61m (2' × 2') luminaire, with a vertically oriented interchangeable optical material. The optical material is backlit by a motorized LED array that can be moved closer to, or further from, the optical material (see Section 2.2). The MDB facilitates automated characterization of the two-dimensional luminance pattern of the UUTB with multiple types of measurement devices and methods (see Section 2.3). The UUTB and MDB are mechanically connected with ancillary adjoining components to facilitate positioning but these adjoining components may be removed so that the bisections can be operated independently. The apparatus may be manually reconfigured such that the UUTB can operate independently for human perception studies or have the MDB placed a set distance from the luminaire aperture.

### 2.1) UNIFIED CONTROL MODULE (UCM)

To ensure that both the UUTB and MDB may operate independently, the UCM (Figure 2) was developed so that power, data, and software remained portable and reconfigurable. The UCM is approximately 0.46m (18.0") wide × 0.23m (9.0") deep × 0.31m (12.0") tall and can be placed on folding shelves on the side of either the UUTB or MDB. The UCM permits all power and data requirements of the system to be provided with a single 120 VAC power feed to the UCM plus a single low voltage cable connection between the UCM and each bisection. Isolating 120 VAC to the UCM enables safer maintenance, modification, and troubleshooting of the bisections.

*Figure 2. Unified Control Module (UCM).*

Hosting both power and data, the two cables between the UUTB, MDB, and UCM are 16 pairs of 16 AWG conductors with individual and overall shielding. The UCM supports varying sizes of power supplies and control hardware, with a DIN rail to enable quick changes to components. A fan is installed for internal temperature regulation, controlled via pulse width modulation to reduce noise and vibration.

### 2.2) UNIT UNDER TEST BISECTION (UUTB)

The UUTB (Figure 3) is 0.98m (38.5") wide × 0.64m (25.0") deep × 1.58m (62.3") tall. The UUTB consists of an upper portion housing an LED array and a cabinet providing support. The upper portion of UUTB was designed to enclose a vertically oriented 0.61m (24.0") square optical material, simulating a typical architectural luminaire. The luminaire aperture area of the UUTB is 0.59m (23.2”) square. The cabinet was sized to position the center of the LED array at 1.25m (49.0") above the floor, corresponding to a selected average adult seated eye height (United States Air Force Research Lab, 2002).

The optical material under evaluation is housed in a vertical metal frame with a removable top cap, examples shown in Figure 4, so the material can be quickly interchanged to vary the stimuli. To avoid reflections off metallic components within the enclosure that could cause unintended light propagation, black shrouds were placed such that reflective components are not exposed to the area between the LEDs and optical material. These shrouds may be interchanged or coated in white tape to simulate the interior finish of a luminaire.

*Figure 3. Unit Under Test Bisection (UUTB).*

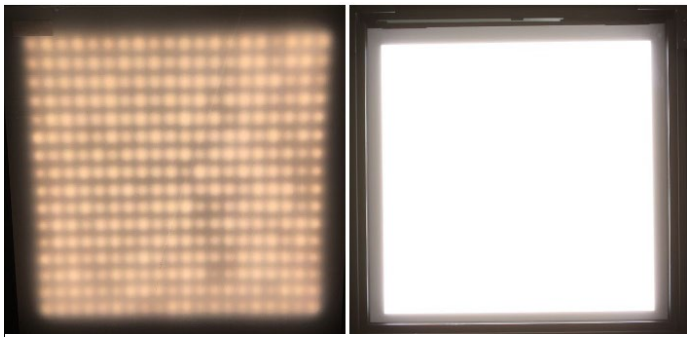

*Figure 4. Examples of visual stimuli.*

*Figure 5. Extents of LED array travel.*

A 0.68m (26.75") wide × 0.61m (24.00") tall × 0.0032m 0.13" thick aluminum plate was fabricated as a mounting surface and heat sink for LED arrays. Its position in the UUTB is controlled by two horizontally oriented Gulfcoast Robotics 350MM TR8X8 lead screw NEMA 17 stepper motors with step size of 0.03mm, and unpublished accuracy and repeatability. This system enables positioning of an LED array at any distance between 0.25m (10.0”) and 0.01m (0.50”) from the optical material emission surface (Figure 5). The LED array may have the position and luminance adjusted via pre-programmed execution or digital control via the UCM. A variety of LED configurations may be mounted to the aluminum plate. Fans are installed in the UUTB to manage heat within the enclosure, with the same control method as the UCM. Any area of the aluminum plate unobscured by an LED array may be covered in white or black tape, as desired, to mimic the interior finish of a luminaire.

### 2.3) MEASUREMENT DEVICE BISECTION (MDB)

The MDB (Figure 7) is 0.98m (38.5") wide by 0.75m (29.5") deep by 1.58m (61.3") tall. The MDB consists of an upper portion housing the gimbal, a lower cabinet portion, and a Connector Conversion Module (CCM). The upper portion is an advanced platform for taking pre-programmed, precisely positioned measurements using multiple devices mounted concurrently, such as a luminance meter, spectroradiometer, and high dynamic range imaging

(HDRI) camera (also known as an array detector or imaging luminance measuring device [ILMD]). While a tripod could be used to position any one measurement device in a specified location, the MDB allows rapid sequential measurements with multiple devices from the same measurement point (measured from each device's sensor position). Utilizing camera posts as a mounting method would usually introduce uncertainty due to difficulty obtaining exact rotational position on the camera post. To resolve this, 3D printed cradles were fabricated to ensure the device's orientation is consistent. The MDB could be considered an evolution of and expansion upon a basic motorized luminance measurement device developed by researchers at the Bartlett School of London in 1984 (Rowlands, et al., 1984), which was used to measure an entire room's luminance from a pivot point, comparing luminance received at an observation point to human subject perceptual responses to the same environment (Loe, et al., 1994).

*Figure 6. Measurement Device Bisection (MDB).*

The CCM (Figure 9) transitions from the single connector between the UCM and MDB to the individual cable connections required for each measurement device. This modularity is intended to enable the apparatus to retain functionality in a variety of potential configurations, while expediting the set-up and execution process by eliminating all but one cable connection. This CCM is inserted into an opening in the side of the lower cabinet portion.

*Figure 7. Connector Conversion Module (CCM).*

### 2.3.1) GIMBAL ASSEMBLY AND ACCURACY

The gimbal assembly (Figure 8) was engineered and manufactured by Zaber Technologies. It is mounted upon an aluminum base plate and centered within the upper portion of the MDB, which shrouds the measurement equipment from stray light and mechanical interference. The upper portion is fastened to the lower cabinet, allowing the ancillary adjoining components to facilitate mechanical alignment of the gimbal pivot point with the center of the UUTB luminaire aperture, at a minimum distance of 0.41m (16"). The upper and lower portions have a cable path between them, allowing larger measurement devices to be placed in the cabinet below with an optical cable connection to the measurement collection remote head on the gimbal.

The gimbal consists of three motorized stages, two of which create rotating motion, while the third creates a translational motion. The two rotating stages enable a series of preprogrammed measurements in a field of view spanning 360° in two dimensions (4π steradians). Each measurement device has positions appropriate for that device pre-programmed in the UCM. The rotating stages have an overall unidirectional accuracy of ± 0.01°, step size of $1.5\times10^{-4}$° and repeatability of < 0.005°. However, each rotating stage only intends to rotate up to 30°, which has a conservative unidirectional accuracy of ± 0.004°. Since repeatability exceeds this accuracy, the uncertainty from accuracy and repeatability is ± 0.005°. A horizontal stage is mounted to the gimbal and moves a platform on which measurement devices are mounted. It has unidirectional accuracy of ± 7.5 µm, step size of 0.048 µm, and repeatability of < 2.5 µm. The combined uncertainty from accuracy and repeatability is ± 7.5 µm. The horizontal stage allows each device to collect measurements from the same pivot point. For simplicity, the following calculations ignore other minor sources of stage position uncertainty, such as wobble.

*Figure 8. Gimbal assembly.*

Gimbal measurement position accuracy is compared to human visual system resolution accuracy (HVSRA) in Table 1. The approximate HVSRA values are estimated from the Illuminating Engineering Society of North America (IESNA) Lighting Handbook, Figure 4.11 (DiLaura, et al., 2011). Equations 1 and 2 are illustrated in Figure 9, and Equations 3 through 7 are illustrated in Figure 10. Equation 1 determines the distance between the gimbal pivot point and the furthest target position (corner of the luminaire aperture) $c_{target}$ or the center of a luminaire aperture edge $c_{edge}$ in microns, where $a_{target}$ and $a_{edge}$ are the distance between the center of the luminaire aperture and the target position in microns ($a_{target}$ = 416,684 µm, $a_{edge}$ = 294,640 µm), and $b_{center}$ is the distance between the measurement device and the luminaire aperture center, in microns. Equation 2 then determines the angle $\angle\alpha_{target}$ or $\angle\alpha_{edge}$ that subtends the center of the luminaire aperture and the target position or edge, in degrees.

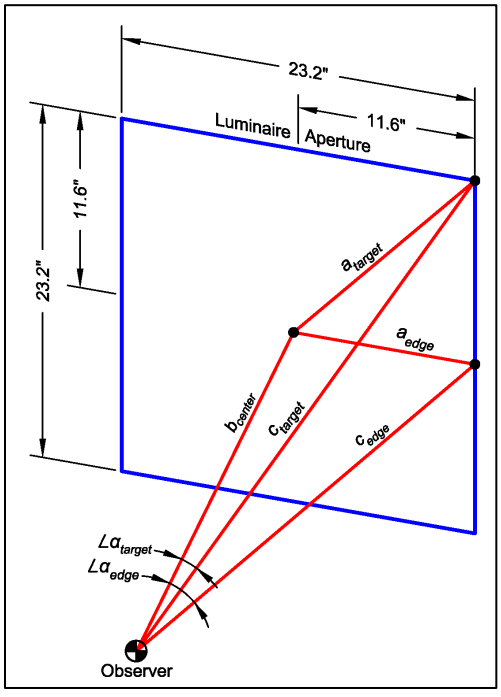


*Figure 9. Equations 1 and 2.*

$$\sqrt{\left(a_{target} \mid a_{edge}\right)^2 + b_{center}^2} = c_{target} \mid c_{edge} \quad (1)$$

$$\angle\alpha_{target} \mid \angle\alpha_{edge} = \tan^{-1}\left(\frac{a_{target}}{b_{center}}\right) \quad (2)$$

*Table 1: Gimbal uncertainty compared to human visual system resolution acuity.*

| Uncertainty compared to HVSRA @ Center of Luminaire Aperture | | | | | |
|---|---|---|---|---|---|
| **Source** | **Description / Variable** | **Values** | | | |
| - | $b_{center}$ Measurement Distance (µm) | 500,000 | 1,000,000 | 1,500,000 | 2,000,000 |
| - | Center of Luminaire Aperture (degree) | 0.000 | | | |
| DiLaura 2011 | HVSRA, Foveal (arcmin) | 1.000 | | | |
| - | HVSRA, Foveal (degree) | 0.017 | | | |
| Zaber | $\angle\alpha_{FOV}$ Rotating Stage Uncertainty (degree) | 0.010 | | | |
| Equation 3 | $r$ for HVSRA, Foveal (± µm) | 72.722 | 145.444 | 218.166 | 290.888 |
| Equation 3 | $r$ for Rotating Stages (µm) | 43.633 | 87.266 | 130.900 | 174.533 |
| Equation 4 | $\angle\alpha_{roterr}$ for Rotating Stages (degree) | 0.005 | 0.005 | 0.005 | 0.005 |
| Equation 5 | $a_{roterr}$ for Rotating Stage (µm) | 43.633 | 87.266 | 130.900 | 174.533 |
| Equation 7 | $a_{linerr}$ for Linear Stages (µm) | 7.500 | | | |
| Equation 8 | $a_{\sum}$ Total Uncertainty (± µm) | 69.207 | 130.913 | 192.620 | 254.327 |
| **Uncertainty compared to HVSRA @ Corner of Luminaire Aperture** | | | | | |
| **Source** | **Description / Variable** | **Values** | | | |
| Equation 1 | $c_{target}$ Measurement Distance (µm) | 650,865 | 1,083,340 | 1,556,800 | 2,042,945 |
| Equation 1 | $c_{edge}$ (µm) | 580,356 | 1,042,503 | 1,528,664 | 2,021,587 |
| Equation 2 | $\angle\alpha_{target}$ (degree) | 39.807 | 22.621 | 15.525 | 11.769 |
| Equation 2 | $\angle\alpha_{edge}$ (degrees) | 30.510 | 16.417 | 11.113 | 8.381 |
| DiLaura 2011 | HVSRA, Peripheral (arcmin) | 8.000 | 3.000 | 2.500 | 2.000 |
| - | HVSRA, Peripheral (degree) | 0.133 | 0.050 | 0.042 | 0.033 |
| Zaber | $\angle\alpha_{FOV}$ Rotating Stage Uncertainty (degree) | 0.010 | | | |
| Equation 3 | $r$ for HVSRA, Peripheral (± µm) | 757.316 | 472.696 | 566.068 | 594.269 |
| Equation 3 | $r$ for Rotating Stages (µm) | 56.799 | 94.539 | 135.856 | 178.281 |
| Equation 4 | $\angle\alpha_{roterr}$ for Rotating Stages (degree) | 30.515 | 16.422 | 11.118 | 8.386 |
| Equation 5 | $a_{roterr}$ for Rotating Stage (µm) | 58.788 | 94.845 | 135.953 | 178.323 |
| Equation 7 | $a_{linerr}$ for Linear Stages (µm) | 8.705 | 7.819 | 7.643 | 7.581 |
| Equation 8 | $a_{\sum}$ Total Uncertainty (± µm) | 91.844 | 141.950 | 199.909 | 259.768 |

Equation 3 calculates the radius $r$ of the HVSRA (using $c_{target}$) or the rotating stage uncertainty (using $c_{edge}$) in microns, where $\angle\alpha_{FOV}$ is the HVSRA at $\angle\alpha_{target}$ or for rotation stages the total uncertainty (0.01°), in degrees.

$$r = \left(c_{target} \mid c_{edge}\right) \times \sin\left(\frac{\angle\alpha_{FOV}}{2}\right) \tag{3}$$

All stage position uncertainty results in a difference in distance between the measurement device and the luminaire aperture. The potential difference in angle between center of the luminaire aperture and the actual position $\angle\alpha_{roterr}$, in degrees, is calculated with Equation 4.

$$\angle\alpha_{roterr} = \tan^{-1}\left(\frac{r}{c_{target}}\right) + \angle\alpha_{edge} \tag{4}$$

Equation 5 then calculates the position error on the luminaire aperture plane as a result of one rotation stage's uncertainty $a_{roterr}$ in microns.

$$a_{roterr} = (b_{center} \times \tan(\angle\alpha_{roterr})) - a_{edge} \tag{5}$$

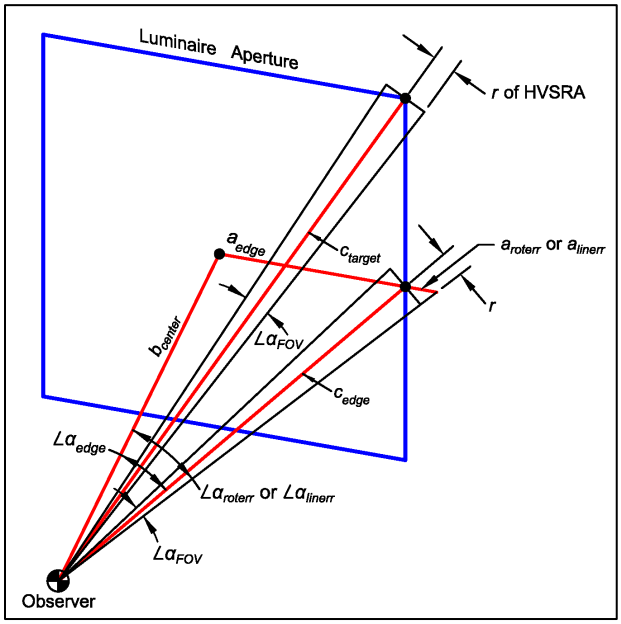


*Figure 10. Equations 3 through 7.*

For the sake of simplicity, it is assumed that linear stage position uncertainty does not result in the measurement device moving off the pivot point, since the uncertainty from this source is negligible. Equation 6 calculates the change in angle $\angle\alpha_{linerr}$ resulting from positioning uncertainty, in degrees, where $x_{acc}$ is the linear stage unidirectional accuracy, in microns (7.5 µm).

$$\angle\alpha_{linerr} = \tan^{-1}\left(\frac{x_{acc}}{c_{edge}}\right) + \angle\alpha_{edge} \tag{6}$$

Equation 7 determines the difference in distance $a_{linerr}$ between $a_{target}$ and $\angle\alpha_{linerr}$, in microns.

$$a_{linerr} = (b_{center} \times \tan(\angle\alpha_{linerr})) - a_{edge} \tag{7}$$

The uncertainty of the three stages is not additive, rather, Equation 8 calculates the combined measurement position uncertainty $a_{\sum}$ in microns, where $a_{roterr}$ is the result from Equation 5 for the horizontal and vertical axis rotating stages and $a_{linerr}$ is the result from Equation 7 for the linear stage.

$$a_{\sum} = \sqrt{2a_{roterr}^2} + a_{linerr} \tag{8}$$

Measurement position uncertainty below the HVSRA is achieved throughout the field of view occupied by a luminaire aperture, as shown in Table 1. For example, at a $b_{center}$ measurement distance of 1,000,000 µm, Equation 3 provides a value of $r$ for foveal HVSRA of ±145.444µm, while Equation 8 results in a lower value for $a_{\sum}$ of ±130.913µm. The rows with the values to be compared are highlighted accordingly. The results illustrate that the apparatus can accurately position a measurement device such that it can provide position fidelity, and thus data fidelity, equal to or greater than the HVSRA, potentially validating lower fidelity methods. In addition,

the results enable the assumption that the measurement position is equal to the target position for future luminance uniformity calculations since position error is not discernable to the human visual system.

## 3) CONCLUSIONS

The LLUA has been designed to investigate the human perception of luminaire luminance uniformity in the context of architectural lighting. The UUTB's stimulus variability provides a high degree of flexibility for creating visual stimuli, and the MDB allows for rapid and accurate characterization of the stimulus with a variety of measurement methods and devices. This combination permits extensive investigation into new and existing luminance uniformity metrics for architectural lighting and for establishing the relationship between these metrics and human perceptions. Stimuli can be repeated for multiple measurement devices, methods, and human psychophysical experiments. The apparatus is also configured for future flexibility such that a variety of improvements and additional research trajectories can be accommodated.

## 4) ACKNOWLEDGEMENTS

The authors acknowledge the contributions of Sarah Safranek (PNNL), who contributed expertise on the use of HDRI in lighting research, Justin Day (PNNL), who conducted a literature review. This work was supported by the U.S. Department of Energy's Lighting R&D Program, part of the Building Technologies Office within the Office of Energy Efficiency and Renewable Energy.

## 5) REFERENCES

Ashdown, I., 2013. Luminance Gradients: Photometric Analysis and Perceptual Reproduction. *LEUKOS,* 25(1), pp. 69-82.

Davis, R. G. & Spring, C. O., 2007. *Metrics of Perception: Luminance Uniformity.* Phoenix, AZ, IESNA, pp. 186-205.

DiLaura, D. L., Houser, K. W., Mistrick, R. G. & Steffy, G. R., 2011. *The Lighting Handbook.* 10th ed. New York, NY: IESNA.

Downen, P., 2006. A closer look at flat-panel-display measurement standards and trends. *Information Display*, January, pp. 16-21.

EBU, 2008. *Methods for the Measurement of the Performance of Studio Monitors.* Geneva: EBU.

Inanici, M. N., 2006. Evaluation of high dynamic range photography as a luminance data acquisition system. *Lighting Research and Technology,* 38(2), pp. 123-136.

Irvin, L., Bermudez, E. R.-F., Feagin, B. & Royer, M., 2020. *Developing High Dynamic Range Imaging Procedures for Luminance Uniformity Measurement.* New Orleans, LA, Submitted to IES Annual Conference Proceedings.

ISO, 2001. *ISO 13406-2:2001 Ergonomic requirements for work with visual displays based on flat panels — Part 2: Ergonomic requirements for flat panel displays,* Vernier, Geneva, Switzerland: ISO.

ISO, 2008. *ISO 9241-305:2008 Ergonomics of human-system interaction — Part 305: Optical laboratory test methods for electronic visual displays,* Vernier, Geneva, Switzerland: ISO.

Loe, D. L., Mansfield, K. P. & Rowlands, E., 1994. Appearance of lit environment and its relevance in lighting design: Experimental study. *Lighting Research and Technology,* 26(3), pp. 119-133.

Moreno, I., 2010. Illumination uniformity assessment based on human vision. *Optics Letters,* 35(23), pp. 4030-4032.

Rowlands, E., Loe, D. L. & Brickman, N. T., 1984. *Instrumentation for Measuring the Luminance Distribution Within the Visual Field.* Cambridge, London, CIBS National Lighting Conference, pp. 187-192.

Safranek, S. & Davis, R. G., 2020. Sources of Error in HDRI for Luminance Measurement: A Review of the Literature. *LEUKOS,* pp. 1-13.

SID, 2012. *Information Display Measurement Standard Version 1.03.* Campbell, CA: SID.

SPWG, 2005. *SPWG Notebook Panel Specification, Version 3.5,* Milpitas, CA: VESA.

Tang, L., 1996. *The Assessment of Ceiling Uniformity for Indirect Lighting Systems.* Troy, NY, Rensselaer Polytechnic Institute.

TSO, 2005. *TCO Certified Notebooks,* Stockholm, Sweden: TCO.

United States Air Force Research Lab, 2002. *CAESAR: Summary Statistics for the Adult Population (Ages 18-65) of the United States of America,* Wright-Patterson AFB, OH: National Technical Information Service.

VESA, 2001. *Flat Panel Display Measurements Standard, Version 2.0,* Milpitas, CA: VESA.

Wang, Q. & Davis, R. G., 1996. A Study on New Beam Parameters. *LEUKOS,* pp. 100-111.

Yao, Q., Zhong, B., Shi, Y. & Ju, J., 2017. Evaluation of Several Different Types of Uniformity Metrics and Their Correlation with Subjective Perceptions. *LEUKOS,* 13(1), pp. 33-45.

Yu, H.-L. & Chung, Z.-Y. C., 2011. Luminance measurement of curved surface sources. *Metrologia,* 48(5), pp. 408-416.

Zhang, J. X. & Ngai, P. Y., 1993. *On Perceptual Preference for Surface Luminance.* Houston, TX, IESNA, pp. 493-521.